

# Improvement in Accuracy of Failure Prediction in FE Simulations of Sheet Metal Forming of Al Alloys

B Prajeesh<sup>1</sup>, D Raja Satish<sup>2\*</sup>, D Ravi Kumar<sup>3</sup>

<sup>1</sup>BHEL Trichy, Tiruchirappalli, Tamilnadu, 10016, prajeesh@bheltry.co.in.

<sup>2\*</sup>Department of Mechanical Engineering, IIT Delhi, New Delhi, 110016, srdometi@gmail.com

<sup>3</sup>Department of Mechanical Engineering, IIT Delhi, New Delhi, 110016, dravi@mech.iitd.ac.in

## Abstract

In this work, the plane strain intercept on the forming limit diagram (FLD<sub>0</sub>) which is the major strain value when the minor strain is zero, has been determined for some important aluminium alloys with a wide variation in grade, heat treatment and thickness through stretch forming experiments. A new correlation between formability parameters (thickness, strain hardening exponent and normal anisotropy) and plane strain intercept in the forming limit diagram has been developed and it is used to generate forming limit diagrams (FLDs) of these alloys in the post processor of FE software. FLDs generated using the developed correlation have been found to be much closer to the experimental FLDs when compared to the FLDs generated in the post processor based on the existing correlation. This has led to significant improvement in accuracy of failure predictions (in terms of limiting dome height and failure strains) in the case of aluminium alloys.

**Keywords:** Aluminium alloys, Forming Limit Diagram, Failure Prediction, FE Simulations

## 1 Introduction

Sheet metal forming is a process in which flat thin blanks are deformed permanently to produce a wide range of products i.e. very simple sheet metal parts to complex three dimensional objects. These operations are widely used in industry and hence knowledge of various sheet metal forming processes is essential to manufacture good quality products. Common parts made by sheet metal forming processes include automobile body panels, fuel tanks, aircraft parts, various parts for building industries and also for making domestic home appliances, food and drink cans.

Aluminium alloys are now-a-days replacing the steel in automobile industry since they have lower weight, comparable strength and high corrosion resistance and they reduce the vehicle weight and hence able to achieve better fuel consumption[Roth et al. 2001]. Large number of aluminium alloy sheets has been developed in the recent past for potential application in automotive industry.

The experimental determination of forming behavior of these modern materials is time consuming which necessitates some easier methods of determining formability. Finite element simulation or theoretical methods are finding wider importance now-a-days. This

can lead to the optimization of process and design variables to achieve better quality stampings.

Forming Limit Diagrams (FLDs)[Keeler and Goodwin, 1971] are widely used in sheet metal stampings for prevention as well as diagnostics of failure. FLDs are also used as a tool to predict failure in simulation of sheet metal forming processes based on the finite element method. The accuracy of failure prediction in FE simulations depends on the accuracy of determined/predicted limit strains of the material. In FE softwares, the FLD is predicted by means of an empirical correlation between plane strain FLD value and material parameters such as strain hardening exponent and thickness of the sheet.

However, predictions based on the correlation have been found to be in poor agreement in the case of Al alloys. Therefore in this work, a new correlation has been developed for calculating the plane strain intercept on the forming limit diagram (FLD<sub>0</sub>) which is used to predict failure in Al alloys.

## 2 Experimental work

The experimental work carried out for determining the tensile properties, formability parameters, limiting dome height and forming limit strains of aluminium alloys.

## 2.1 Material selection

Aluminium alloys of different series like 6xxx, 2xxx, and 7xxx having thickness range 0.5-1.6 mm in different tempers were used for studying the effect of thickness and material properties on the FLD.

## 2.2 Determination of tensile properties

The tensile properties of the materials were tested as per ASTM standard E8M. The specimens were prepared by laser cutting in three directions with the length parallel ( $0^\circ$ ), diagonal ( $45^\circ$ ) and perpendicular ( $90^\circ$ ) to the rolling direction of the sheet.

The specimens were tested in uniaxial tension on Instron machine at a constant cross head speed of 5 mm/min. The tested and untested tensile samples are shown in Figure 1. Load elongation data was obtained for all the tests which were converted into engineering stress strain curves. The standard tensile properties such as yield stress, ultimate tensile stress, uniform elongation and total elongation were determined from the stress-strain data. Strain hardening exponent and strength coefficient were obtained by converting the engineering stress strain into true stress strain data.



Figure 1: Tensile samples

The plastic strain ratio, which is a measure of anisotropy, was determined using specimens prepared according to ASTM E517 specification. The specimens were elongated to a predetermined longitudinal strain (10% and 15% depending on the % elongation up to ultimate tensile strength) and the test was stopped before the onset of necking. Final width and gauge length were measured and the plastic strain ratio ( $R$ ) was calculated as the ratio of true strain in width direction to true strain in thickness direction [Hosford and Caddell, 1983].

The  $R$  value was determined in three directions as mentioned in the tensile tests by repeating the above procedure. The normal anisotropy or average plastic strain ratio ( $\bar{R}$ ) was calculated.

## 2.3 Experimental determination of FLDs of Al alloy sheets

As suggested by Hecker [1974], samples of varying width were deformed using a 101.6 mm diameter hemispherical punch. The width was varied to obtain all possible deformation modes i.e. biaxial tension, plane strain tension and tension-compression. The schematic diagram of the arrangement of tools used in experiments is shown in Figure 2.

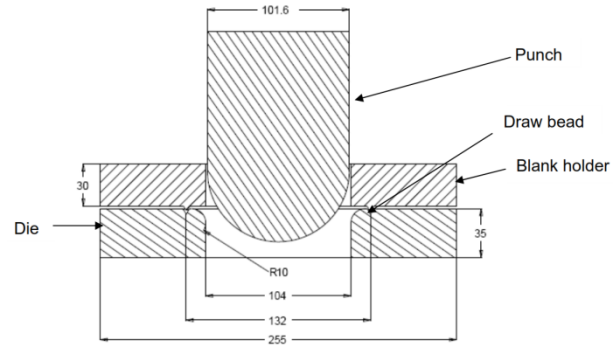


Figure 2: Schematic diagram of the arrangement of tools used in FLD tests.

A 101.6 mm diameter punch was used with dies (lower die and blank holder) having a draw bead to prevent the drawing in of the blank for certain widths. The draw bead ensures that only portion of blank within the die region is stretched completely without drawing. The sheet strips of varying widths were clamped firmly between the die and the blank holder before they were stretched over the punch. The extent of drawing in during punch stretching depends on the width of the blank. As the width decreases the drawing component increases and stretching component decreases. The samples of width varying from 125 mm to 175 mm with constant length (175 mm) were used to get data in biaxial tension region. Samples having 25, 50 and 75 mm width were used for strain data with negative minor strain. These blanks were cut with length perpendicular to the rolling direction. The blanks were laser marked with 5 mm diameter circles with a gap of 0.5 mm between the circles. Samples of 100 mm width were found to give zero minor strains (plane strain condition).

The grid marked specimens were deformed using a double action hydraulic press of 100-tonne capacity. The specimen was placed between the upper and lower dies. An optimum blank holding force in the range of 1-1.5 tons was applied on the upper die to clamp the blank at the draw bead. The experiment was stopped once a visible neck or initiation of fracture was obtained on the specimen.

Major and minor principal strains were calculated by measuring major and minor diameters of ellipses on

the deformed samples. A travelling microscope having a least count of 0.001mm was used to measure major and minor diameters of ellipses for strain calculations. The limited dome height (LDH) of all the specimens at the point of necking/fracture was measured using a vernier height gauge with a least count of 0.02 mm.

### 3 Results and discussion

#### 3.1 Tensile properties and anisotropy

A typical engineering stress-strain and true stress-strain curve for 6061-O alloy of 1.6mm thickness are shown in Figure 3.

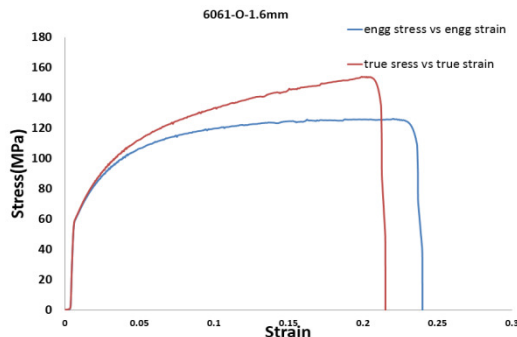


Figure 3: Engineering and true stress strain curve of 6061-O, t=1.6 mm

Tensile properties like yield strength (YS), ultimate tensile strength (UTS), total % elongation, strain hardening exponent (n) and strength coefficient (K) and anisotropy for all grades were determined from the stress-strain data. The properties of 6061-O alloy are given in Table 1 for three different thickness.

Table 1: Material properties and the normal anisotropy value for 6061-O alloy

Grade	Thickness	YS(MPa)	UTS(MPa)	%Eln (GL:50mm)	n	K(MPa)	$\bar{R}$
6061-O	0.5mm	45.86	113.5	24.87	0.301	234.8	0.652
	1mm	50.73	125.2	23.24	0.313	272.4	0.633
	1.6mm	59.86	123.7	27.16	0.267	241.96	0.642

$\bar{R} = (R0+2*R45+R90)/4$

The average plastic strain ratio of all the sheets is low (<1) indicating inferior drawability of these sheets when compared to conventional drawing quality low carbon steel, for which  $\bar{R}$  is usually in the range of 1.4 - 1.8 [Sing, W.M. and Rao, K.P., 1993].

#### 3.2 Determination of Forming Limit Diagrams

Stretch forming tests were conducted by varying widths. The major and minor strains in the safe, necked and failure regions were measured and FLDs were drawn such that strains at necking/fracture lie just at or

above the line. Tested samples in stretch forming are shown in Figure 4 and Figure 5. These FLDs were drawn for all the grades. As an example, FLDs for 6061-O, t=0.5 mm is shown in Figure 6.



Figure 4: Specimens before and after deformation



Figure 5: Necking in the samples

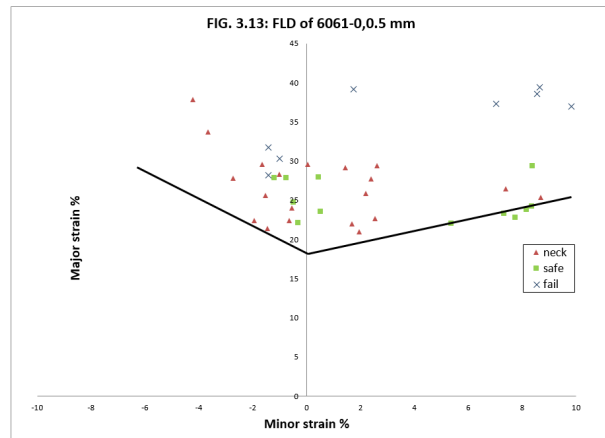


Figure 6: FLD of 6061-O, t=0.5 mm thickness

The FLD<sub>0</sub> values have been found out for all the materials from the experimentally determined FLDs. For example, the FLD<sub>0</sub> of 6061-0 increased from 22.2% to 30.9% as the thickness increases from 0.5 to 1.6mm in the case of aluminium alloys as shown in Table 2.

**Table 2:FLD<sub>0</sub> determined experimentally**

Grade	Thickness(mm)	FLD <sub>0</sub> (%)
6061-O	0.5	18.12
	1	23.9
	1.6	30.92

**3.3 FE simulations**

The FE simulations were done to check the accuracy of failure prediction in stretch forming of aluminium alloys. The failure predictions based on the developed as well as existing correlations were compared with the experimental results.

The stretch forming simulations were carried out using a 101.6 mm hemispherical diameter punch. The dimensions of blanks used are 175mm X 175mm, 175mm X 100mm and 25mm width representing three different modes of deformation namely biaxial stretching, plain strain condition and tension-compression respectively. The punch, die and blank holder were modeled in preprocessor and a circular draw bead of 132 mm diameter was defined on the die. The blank was placed at the center of the die. All tools were considered to be rigid bodies. The blank was considered as a deformable body and it was meshed with quadrilateral shell elements. The default shell element formulation is BELYTSCHKO-TSAY, which is widely implemented in stamping simulation. The arrangement of meshed tools and blank is shown in Figure 7.

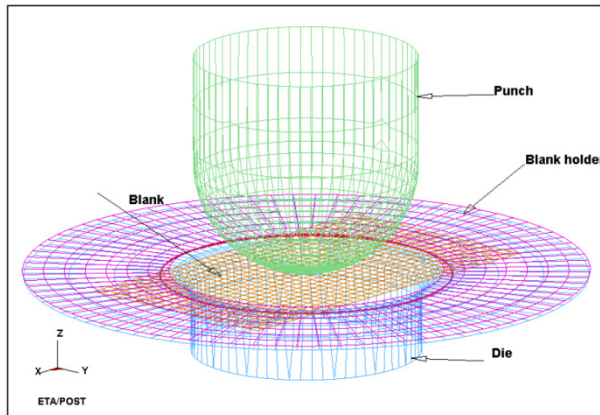


**Figure 7:Arrangement of tools and blank in FE simulation**

Barlat’s three parameter plasticity model[Barlat and Lian, 1989] was used to simulate plastic deformation behavior of blanks during stretch forming. It incorporates the effect of both normal and planar anisotropy. Material is assumed to be rigid plastic with power law of strain hardening. The true stress-true strain curve was given as input to the material library

for performing the simulations. The following process parameters (Table 3) were used in the simulations of the stretch forming of the blanks.

**Table 3:Process parameters used in FE simulations**

Process parameter	Value
Punch travel	40mm
Punch speed	1000mm/sec
Coefficient of friction	0.125
Blank holding force	15000N

**3.3.1 Prediction of failure in FE simulations**

Presently, FLDs are generated in the post processor of DYNAFORM software (with LS DYNA solver) to predict failure in the simulations of sheet metal forming processes. These FLDs are generated using certain correlations to calculate FLD<sub>0</sub> based on the n and t values. The empirical relation (LS DYNA Manual) used in the post processor of LS DYNA is given below.

$$\text{If } t < 0.1'', FLD_0 = \frac{n}{0.21} (23.3 + 359t)$$

$$\text{If } 0, 1'' \leq t \leq 0.21'', FLD_0 = \frac{n}{0.21} (20 + 525t - 1250t^2)$$

$$\text{If } t > 0.21'', FLD_0 = \frac{n}{0.21} \times 20$$

where, t is sheet thickness in inches and n is strain hardening exponent of the sheet.

Based on FLD<sub>0</sub> the value, the whole curve is plotted by offsetting the standard curve of 1 mm low carbon steel. Using these existing correlations, FLDs were generated in the post processor and they are compared with the experimentally determined FLDs.

**3.3.2 Development of new correlation**

It is evident that existing correlation is only valid for low carbon steels. For aluminium alloys there was a huge difference between the predicted FLD and experimental FLD (shown in Figure 8).

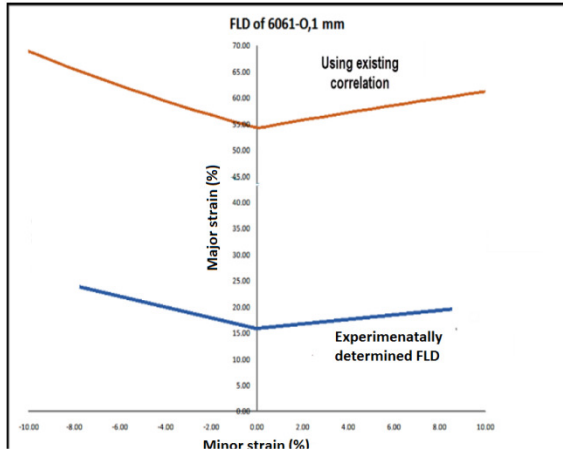


**Figure 8: Comparison of FLD generated from the correlations used in the post processor with the experimentally determined one for 6061-O alloy with 1mm thickness.**

From the Figure 8, it is clear that the FLDs generated from the post processor using the existing correlations predict much higher limit strains as compared to the actual experimental FLD. These predictions exceed the limit strains by 20-30%, which clearly indicates the need for better correlation that can predict more realistic values of  $FLD_0$ .

So multiple regression analysis was performed with thickness, forming properties  $n$  and  $\bar{R}$  as the independent variables and  $FLD_0$  as the dependent variable. Various types of combinations of independent variables were used for performing the regression analysis so as to obtain better results. It is seen that the linear combination of  $t$ ,  $n$  and  $\bar{R}$  can predict the results fairly accurately and the developed correlation is given below:

$$FLD_0 = 2.25t + 48.14n - 35.48\bar{R} + 26.32$$

Where,  $FLD_0$  is in % strain and  $t$  is in mm.

The  $FLD_0$  generated by this correlation has been given as input to the post processor of the FE software which generated the entire curve by offsetting the standard curve in the post processor. The predicted FLD based on the new empirical relation (dashed line) is then compared with the experimentally determined FLD (solid line) as shown in Fig. The FLD generated in the post processor with the developed correlation (dashed line) is far better than the one predicted by existing correlation (dotted line). The slope of the FLD generated by the post processor is good match to the experimentally determined FLD. Comparison between experimentally determined FLD and FLD using developed correlation shown in Figure 9 & Figure 10 gives us good match.

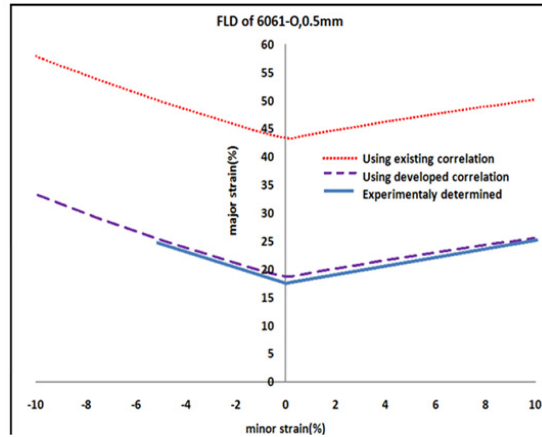


**Figure 9: Comparison of FLD generated from the developed correlations with the experimentally determined and existing correlation used in the post processor for 6061-O alloy, 0.5 mm thickness.**

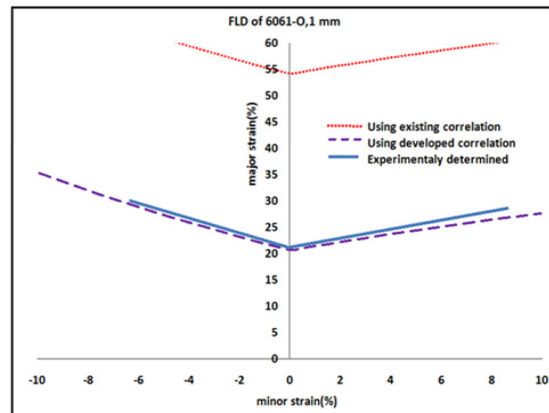


**Figure 10: Comparison of FLD generated from the developed correlations with the experimentally determined and existing correlation used in the post processor for 6061-O alloy, 1 mm thickness.**

Stretch forming of three different types of specimens was simulated using LS DYNA to predict failure and LDH for the cases of biaxial stretching (width 175mm), plane strain condition (width 100mm) and tension-compression (width 25 mm). Initially, the FLD based on the existing correlation was used to predict failure in the postprocessor. The strain data for 2024-O alloy of deformed samples of 175mm width (biaxial stretching) is superimposed on the FLD as shown in Figure 11 at the point of fracture. The LDH has been found to be 54.1 mm which is significantly higher than the experimental LDH (31.9mm). When the FLD based on the developed correlation was used, the predicted LDH is 30.6mm. The strain at failure in this case is shown in Figure 12.

Limiting dome height (LDH) by using FLDs based on existing and developed correlations, are compared with experimental values for three grades (2024-O, 6022-T4, and 2524-T3) in Table 4. It can be clearly seen that there has been a significant improvement in accuracy of prediction of LDH and limit strains when the correlation developed in the present work has been used to calculate  $FLD_0$ . It is expected to be highly beneficial for accurate predictions of failure in the case of aluminium alloys.

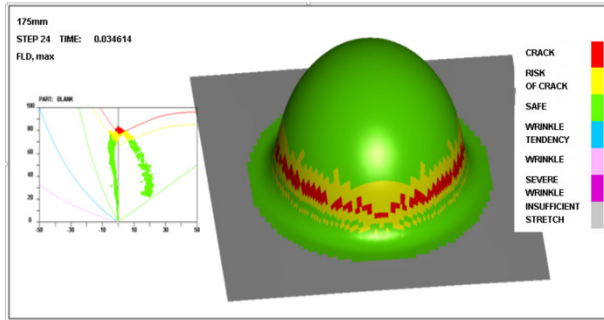


**Figure 11: Failure prediction based on the correlation already presented in LS DYNA for a rectangular specimen of size 175mm X 175mm**

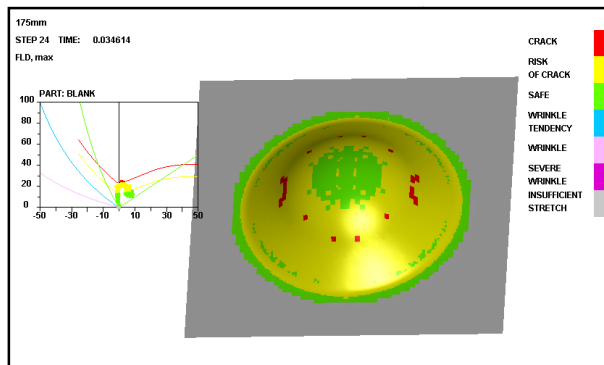


**Figure 12: Failure prediction based on the developed correlation for a rectangular specimen of size 175mm X 175mm**

**Table 4: Comparison of limiting dome height**

Grade	Thickness(mm)	specimen size	Dome height in mm(simulation)		Dome height in mm(Experiments)
			using FLD based on existing correlation	using FLD based on developed correlation	
2024-O	1.6	175X 175	54.1	30.6	31.9
		175 X 100	43.9	30.5	27.6
		175 X 25	51.2	27.6	20.6
6022-T4	1	175X 175	34.6	31.6	31.8
		175 X 100	33.1	28.5	28.2
		175 X 25	26.9	22.6	24.42
2524-T3	0.8	175X 175	29.8	16.32	18.32
		175 X 100	30.7	16.5	24.26
		175 X 25	22.3	14.82	16.2

## 4 Conclusions

It has been found that there is a large discrepancy in the FLDs generated in the post processor of FE softwares based on existing empirical correlations and the experimental FLDs of Al alloys. This leads to a significant error in failure predictions in sheet metal forming of Al alloys using FE simulations. A new correlation has been developed for calculation of plane strain intercept of Forming Limit Diagrams ( ) with material properties and thickness of Al alloys and this correlation has improved the accuracy of failure prediction in FE analysis when compared to the FLDs generated in the post processor of FE software. There has been a significant improvement in accuracy of prediction of limiting dome height and limit strains in FE simulations of sheet deformation in different modes (biaxial stretching, plane strain and tension-compression) when the correlation developed in the present work has been used to plot the FLDs.

## 5 References

- ASTM Standard E517, (2010), Standard Test Method for Plastic Strain Ratio  $r$  for Sheet Metal, *ASTM International*, West Conshohocken, PA, 2003, DOI: 10.1520/E0517-00R10.
- ASTM Standard E8-01, Standard Test Methods for Tension Testing of Metallic Materials, *ASTM International*, West Conshohocken, PA, 2003, DOI: 10.1520/E0008-01.
- Barlat, F., and Lian, J.I. (1989). Plastic Behavior and Stretchability of Sheet Metals, Part-I, *Int. J. Plasticity*, 5, pp. 51-56.
- Hecker S.S (1974), A Reproducible Cup Test for Assessing Sheet Metal Stretchability, *Met. Eng. Q.* 14, pp. 30-36.
- Hosford, W.F. and Caddell, R.M., (1983), Metal forming mechanics and metallurgy, Prentice Hall.
- Keeler S.P., (1971). Understanding sheet metal formability, *Sheet Met. Ind.*, pp. 357-364.
- Roth, R., Clark, J., and Kelkar, A. (2001), Automobile bodies: Can aluminum be an economical alternative to steel?, *JOM. City: Springer-Verlag*, pp. 28-32.
- Sing W.M. & Rao K.P. (1993), Prediction of sheet metal formability by tensile test results, *Journal of Materials Processing Technology*, 37(1-4) pp. 37-51.